Supporting Information

Versatile Direct-Writing of Aerogel-Based Sol-Gel Inks

Jianming Yang‡, Hongqiang Wang‡, Bin Zhou, Jun Shen, Zhihua Zhang and Ai Du**

Shanghai Key Laboratory of Special Artificial Microstructure Materials and Technology, School of Physics Science and Engineering, Tongji University, Shanghai 200092, People's Republic of China

Corresponding authors

*E-mail: zhoubin863@tongji.edu.cn (*Bin Zhou*)

*E-mail: duai@tongji.edu.cn (*Ai Du*)

Table of contents

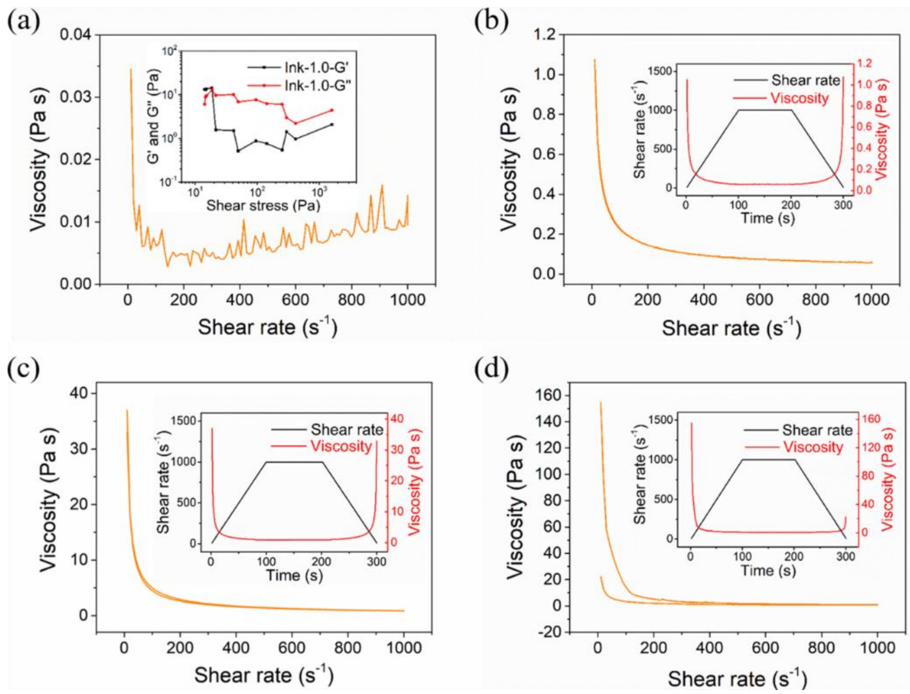

Figure S1. The rheological behaviors and thixotropic behaviors of RA inks: (a) The viscosity as function of the shear rate for Ink-1.0. The illustration shows the storage and loss modulus as functions of the shear stress for Ink-1.0. (b), (c) and (d) The thixotropic behaviors of Ink-1.1, Ink-1.2 and Ink-1.4, respectively. The illustration shows the change of shear rate and viscosity with time during the experiment.

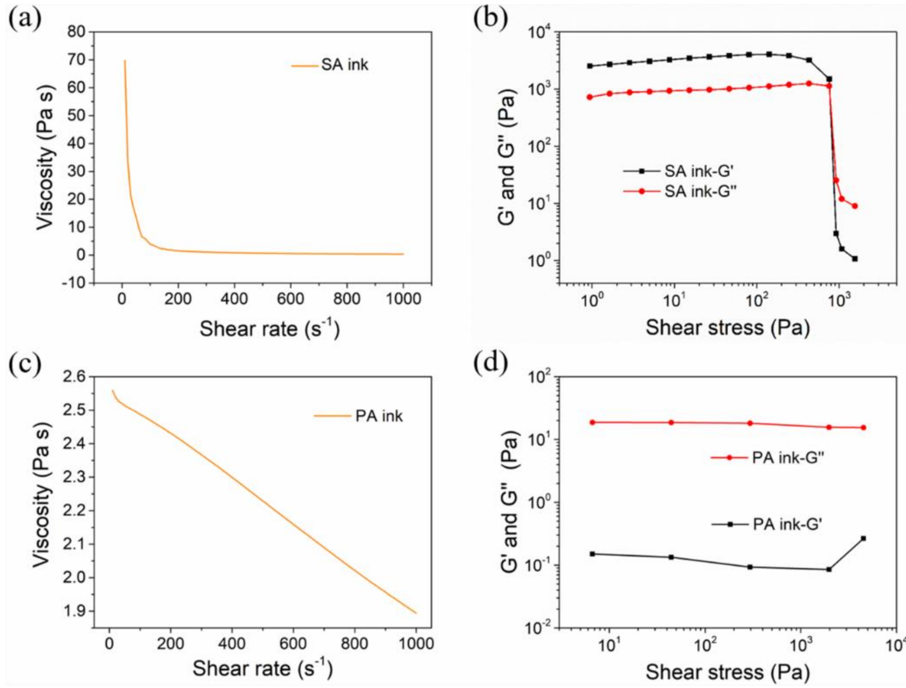

Figure S2. The rheological behaviors of SA ink and PA ink: (a) The viscosity as function of the shear rate for SA ink. (b) The storage and loss modulus as functions of the shear stress for SA ink. (c) The viscosity as function of the shear rate for PA ink. (d) The storage and loss modulus as functions of the shear stress for PA ink.

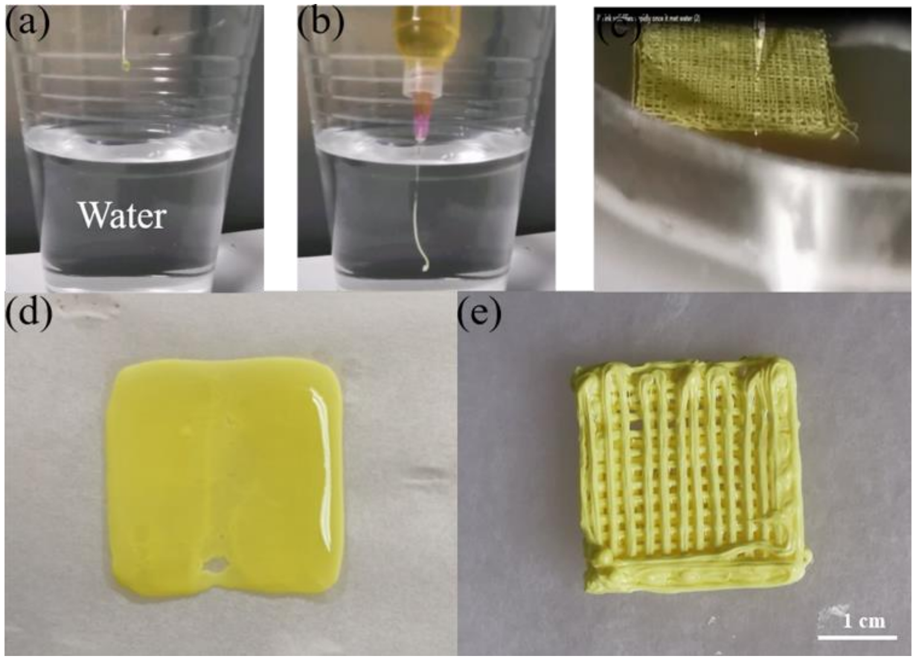

Figure S3. The rapid solidification of PA ink once it met water: The state of PA ink before (a) and after (b) exposure to water, the inner diameter of needle is 410 μm. (c) The printing of PA ink in a water-pool was demonstrated by using a high-precision needle with the inner diameter of 30 μm. The printing of PA ink without (d) and with (e) a water-pool.

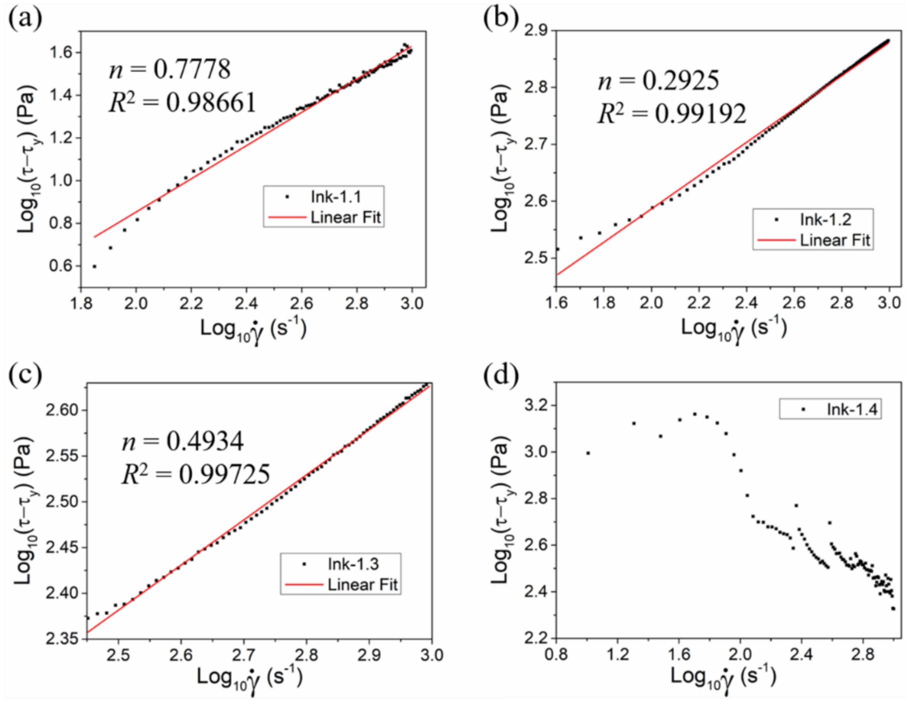

Figure S4. The shear-thinning behaviors were analyzed by the Herschel-Buckley model for Ink-1.1 (a), Ink-1.2 (b), Ink-1.3 (c), and Ink-1.4 (d), respectively. *n* is the shear-thinning index, and R^2 is the fitting determination coefficient.

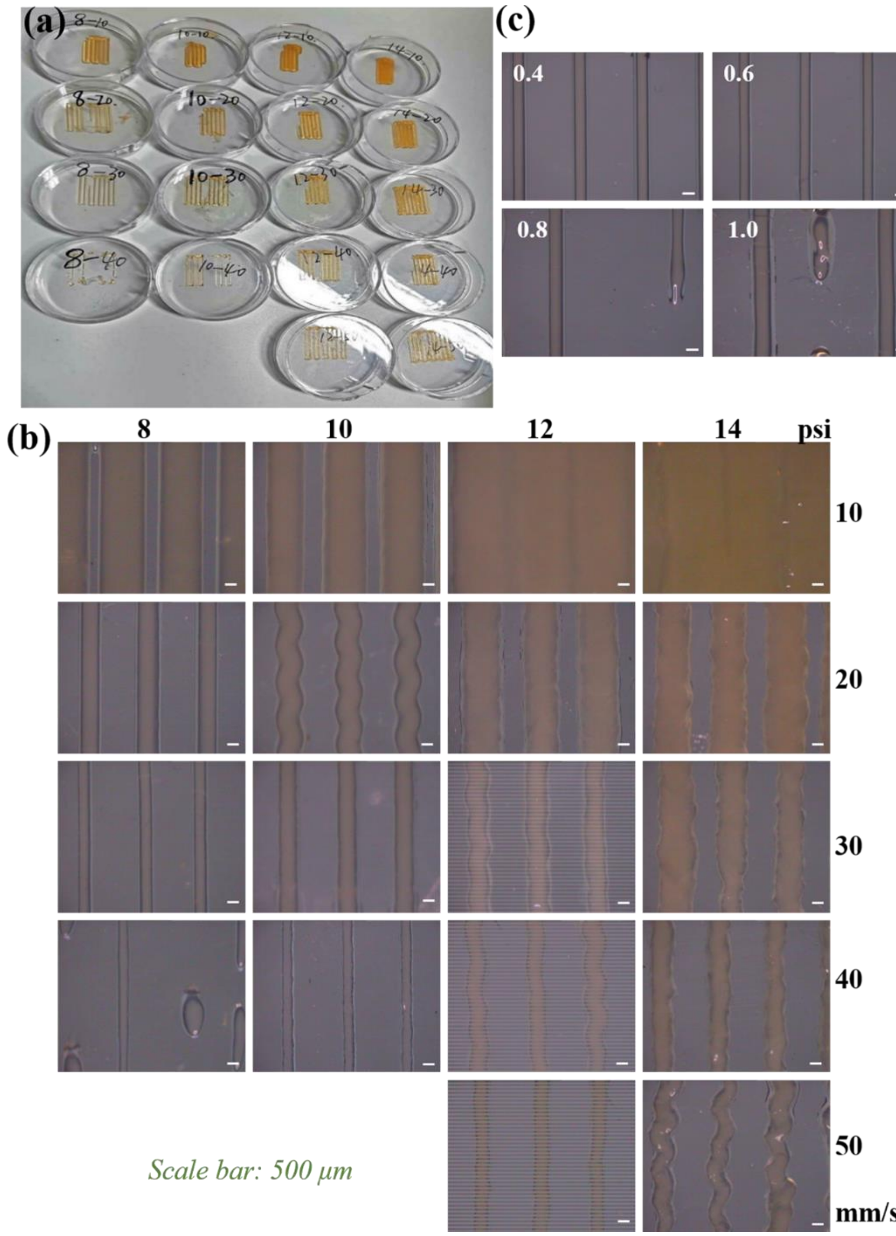

Figure S5. The study of relevant parameters in DIW. (a) Physical images of a single layer printed at varied applied pressures (*P* = 8, 10, 12, and 14 psi, respectively) and writing speeds (*V* = 10, 20, 30, 40, and 50 mm s^{-1}, respectively). (b) Optical microscope images of extruded filaments at varied applied pressures and writing speeds corresponding to (a). (c) Filament widths at varied height of needle to substrate (*H* = 0.4, 0.6, 0.8, and 1.0 mm, respectively), and in constant P (8 psi) and V (30 mm s^{-1}). (b) and (c): the scale bar is 500 μm.

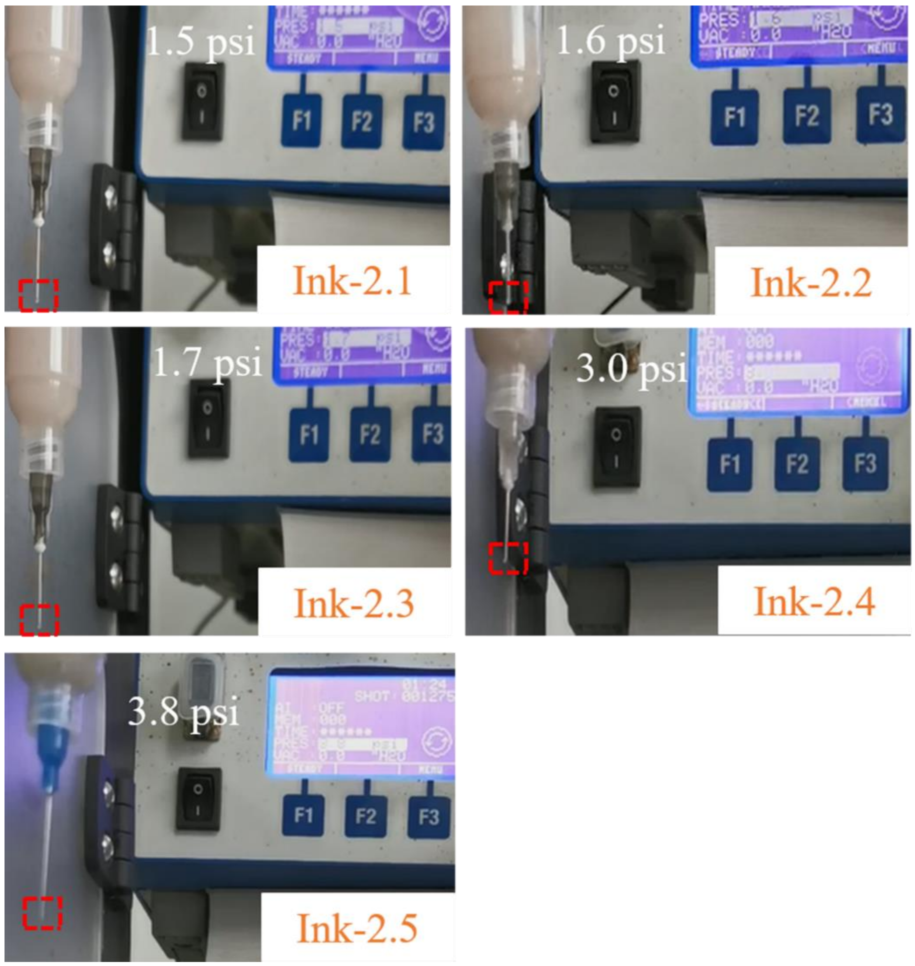

Figure S6. The captures of the experiment measuring the pressures at which the inks are just squeezed out for the dextrin. The red box marked the parts of the inks extruded.

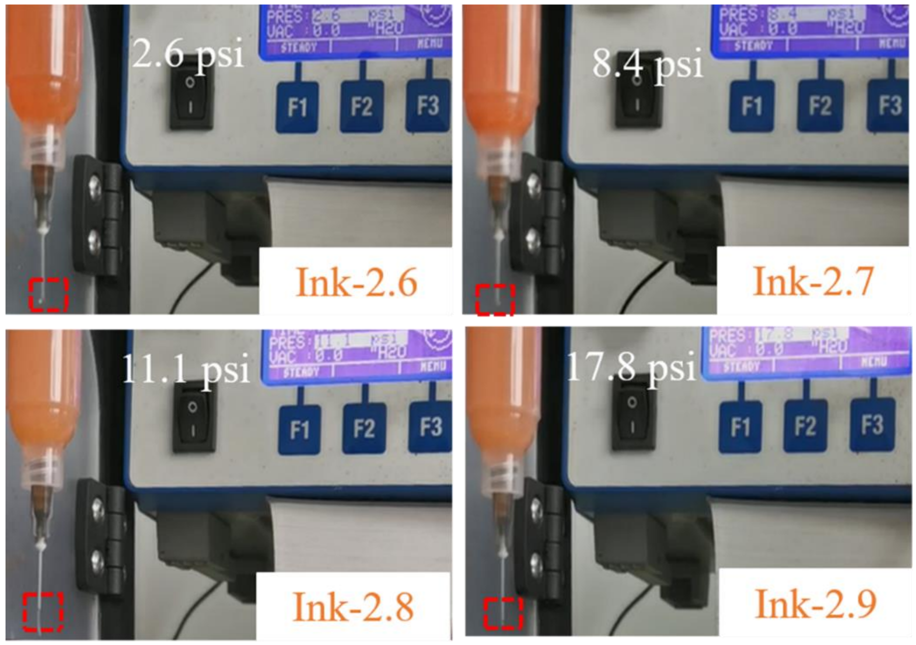

Figure S7. The captures of the experiment measuring the pressures at which the inks are just squeezed out for RA inks. The red box marked the parts of the inks extruded.

3D-printed hydrogels

The 3D meshes with the size of 23.8 mm x 23.8 mm and the distance of 2.2 mm between the bars were printed by 6-layers with RA ink (Figure S8a), by 6-layers with SA ink (Figure S8d), and by 12-layers with PA ink (Figure S8e, f). The 3D meshes with the size of 21.2 mm x 21.2 mm and the distance of 1.2 mm between the bars were printed by 6-layers with RA ink (Figure S8b) and by 6-layers with SA ink (Figure S8c), respectively.

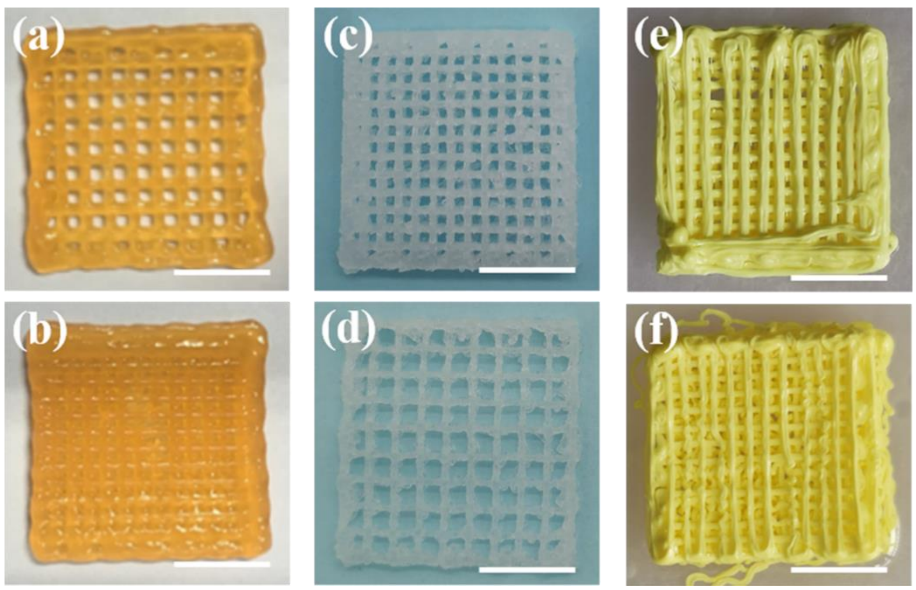

Figure S8. The DIW3DP printed hydrogels by using RA ink, SA ink and PA ink: (a) and (b) RA ink. (c) and (d) SA ink. (e) and (f) PA ink. Scale bar = 1 cm.

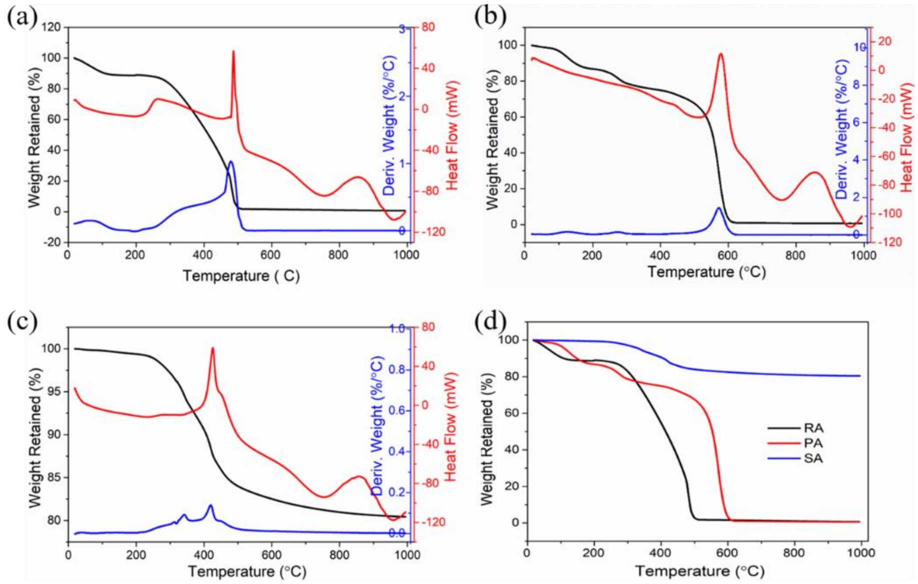

Figure S9. The TG-DSC tests for 3D-printed aerogels. (a) 3D-printed RA. (b) 3D-printed PA. (c) 3D-printed SA. (d) The weight retained (%) of 3D-printed RA, PA and SA.

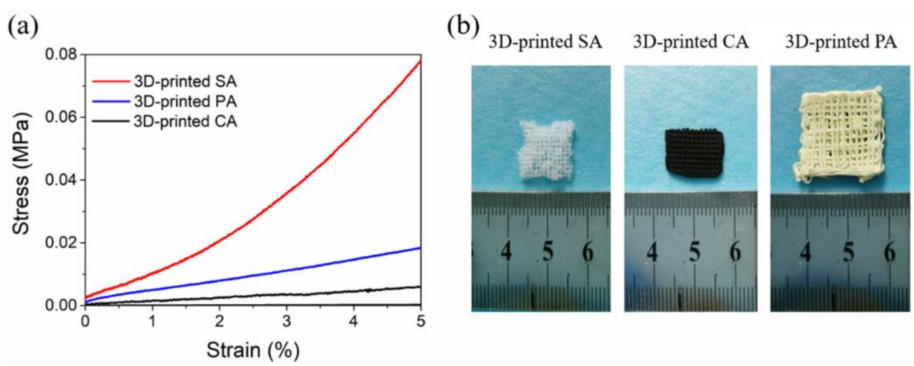

Figure S10. The uniaxial compression-decompression test for 3D-printed aerogels. (a) The stress-strain curves between 0 and 5 %. (b) The pictures of 3D-printed aerogels after uniaxial compression-decompression test.

Derivation of the correlation of the relevant parameters

The applied pressure allows the ink to flow smoothly through the syringe and the needle (Fig. 3(a)). The flowing fluid can be regarded as composed of an infinite number of liquid layers moving in parallel with each other, the slow-flowing liquid layer retards the motion of the fast-flowing one, so that the relative moving shear force is generated between the adjacent liquid layers (Fig. 3(b)). Assuming an insignificant change in viscosity with shear rate inside the syringe and the needle. According to the Hagen-Poiseuille model, differential analysis of the fluid inside the needle yields four forces.

$$F_1 = f = -2\pi r l \eta \frac{dv}{dr} \tag{S1}$$

$$F_2 = f + df = f - 2\pi l \eta d(r\frac{dv}{dr}) \tag{S2}$$

$$F_3 = p_1 2\pi r dr \tag{S3}$$

$$F_4 = p_2 2\pi r dr \tag{S4}$$

where F_1, F_2 are the relative moving shear force between the adjacent liquid layers, respectively; F_3, F_4 are the force generated by the pressure p_1 and p_2, respectively. The fluid is being squeezed out at a constant speed, so we have

$$F_1 - F_2 + F_3 - F_4 = 0 \tag{S5}$$

Plug in equation (S1) - (S4), and we get

$$2\pi l \eta d\left(r\frac{dv}{dr}\right) = -(p_1 - p_2)2\pi r dr \tag{S6}$$

The overall flow velocity close to the needle wall is low and can be idealized to 0. After integrating equation (S6), we can get

$$v = \frac{(p_1 - p_2)}{4l\eta}(R^2 - r^2) \tag{S7}$$

So we can get the volume flow rate of the fluid through the needles

$$Q = \int_0^R v ds = \frac{\pi R^4}{8l\eta}(p_1 - p_2) \tag{S8}$$

where R, l, η and $p_{1 \text{ or } 2}$ are the radius of the needle, the length of the needle, the viscosity of the inks and the pressures at both ends of the needle, respectively. Additionally, the velocity of each layer in laminar flow is different, so a velocity gradient ($\frac{dv}{dr}$) is formed in the radial direction, that is, the shear rate

$$\dot{\gamma} = \frac{dv}{dr} = \frac{(p_1 - p_2)r}{2l\eta} \tag{S9}$$

Finally, according to the relationship between shear stress, viscosity and shear rate, we obtain the shear stress

$$\tau = \eta \cdot \dot{\gamma} = \frac{Pr}{2l} \tag{S10}$$

where r, l and P=$(p_1 - p_2)$ are the distance from the needle center, the length of the needle and the applied pressure, respectively. There exists the maximum shear stress (where r = R=d/2, d is the inner diameter of the needle) according to equation (S10).

$$\tau_{\max} = \frac{Pd}{4l} \tag{S11}$$

Table S1. Filament widths at varied applied pressures and writing speeds.

P(psi)	V(mm s^{-1})	W(mm)					$\overline{\boldsymbol{W}}$(mm)
8	10	1.961	1.947	1.839	1.778	1.711	1.847
8	20	1.036	1.182	1.040	1.037	1.142	1.087
8	30	0.722	0.726	0.706	0.704	0.707	0.713
8	40	0.603	0.623	0.609	0.607	0.601	0.609
10	10	2.048	2.145	2.108	2.086	2.138	2.105
10	20	1.372	1.340	1.349	1.344	1.388	1.359
10	30	1.014	1.003	0.998	0.959	0.927	0.980
10	40	0.561	0.564	0.575	0.552	0.535	0.557
12	10	2.609	2.700	2.759	2.754	2.627	2.690
12	20	1.960	1.891	1.838	1.888	1.819	1.879
12	30	1.161	1.166	1.152	1.144	1.188	1.162
12	40	0.925	0.890	0.895	0.968	0.926	0.921
12	50	0.788	0.771	0.802	0.795	0.810	0.793
14	10	2.871	2.885	2.852	2.880	2.857	2.863
14	20	2.202	1.955	1.931	1.881	1.950	1.984
14	30	1.830	1.529	1.512	1.383	1.495	1.550
14	40	1.074	0.990	1.015	1.050	1.037	1.033
14	50	0.793	1.002	0.947	0.966	0.870	0.916

Table S2. Filament widths at varied height of needle to substrate.

H(mm)			W(mm)			$\overline{\boldsymbol{W}}$(mm)
0.4	0.660	0.664	0.662	0.667	0.665	0.664
0.6	0.596	0.610	0.601	0.612	0.608	0.605
0.8	0.766	0.747	0.746	0.750	0.749	0.752
1.0	0.866	0.862	0.870	0.869	0.872	0.868

Table S3. The pressure value (P), maximum shear stresses (τ_{max}), yield stresses (τ_y), length (l) and inside diameter (d) of needles for extrusion experiments.

Ink-	P/psi	τ_{max}/Pa	τ_y/Pa	l/mm	d/mm
2.1	1.5	81.55	71.51	13	0.41
2.2	1.6	86.98	71.51	13	0.41
2.3	1.7	92.42	71.51	13	0.41
2.4	3.0	83.54	71.51	13	0.21
2.5	3.8	107.42	71.51	25	0.41
2.6	2.6	141.35	114.00	13	0.41
2.7	8.4	456.66	477.80	13	0.41
2.8	11.1	603.45	665.70	13	0.41
2.9	17.8	967.69	981.40	13	0.41

Table S4. Detailed parameters of bulk CA and 3D-printed CAs.

Sample	Bulk CA	3D-printed CA-1	3D-printed CA-2
Diameter (mm)	19.64	23.07	23.69
Diameter (mm)	19.69	22.91	23.24
Diameter (mm)	19.66	23.16	23.01
Average diameter (mm)	19.66	23.05	23.31
Thickness (mm)	2.15	1.75	1.77
Thickness (mm)	2.20	1.93	1.74
Thickness (mm)	2.38	1.72	1.70
Average thickness (mm)	2.24	1.80	1.74
Weight (g)	0.1145	0.1084	0.0662
Density (mg cm^{-3})	168	144	89

Table S5. The water evaporation data of 3D-printed CAs, bulk CA and pure water.

Sample	EV_{sun} (Kg m^{-2} s^{-1})	EV_{dark} (Kg m^{-2} s^{-1})	ΔT (K)	ΔH_{vap} (KJ mol^{-1})	η (%)
Pure water	8.58×10^{-5}	2.39×10^{-5}	5.7	43.6040	15.15
Pure water	8.58×10^{-5}	2.39×10^{-5}	5.7	43.5999	15.14
Pure water	8.58×10^{-5}	2.39×10^{-5}	5.7	43.6040	15.15
Bulk CA	3.37×10^{-4}	4.97×10^{-5}	4.0	43.5339	69.86
Bulk CA	3.37×10^{-4}	4.97×10^{-5}	3.7	43.5298	69.81
Bulk CA	3.37×10^{-4}	4.97×10^{-5}	3.6	43.5256	69.79
3D-printed CA-1	4.03×10^{-4}	5.37×10^{-5}	3.5	43.3136	84.51
3D-printed CA-1	4.03×10^{-4}	5.37×10^{-5}	3.2	43.3080	84.46
3D-printed CA-1	4.03×10^{-4}	5.37×10^{-5}	3.3	43.3065	84.47
3D-printed CA-2	4.35×10^{-4}	6.92×10^{-5}	3.4	43.2337	88.39
3D-printed CA-2	4.35×10^{-4}	6.92×10^{-5}	3.2	43.2416	88.38
3D-printed CA-2	4.35×10^{-4}	6.92×10^{-5}	3.3	43.2249	88.36

EV_{sun}: water evaporation rates under 1 sun illumination; EV_{dark}: water evaporation rates in the darkness; ΔT: water temperature difference after and before solar illumination; ΔH_{vap}: the latent heat of vaporization; η: evaporation efficiency.